



BOSE INSTITUTE

PROJECT REPORT SUBMITTED FOR THE DEGREE  
OF MASTER OF SCIENCE

# Development of Resistive Plate Chamber (RPC) for CBM Muon Chamber

*by*  
Sayan Chakraborty  
Roll No-09

supervised by  
Dr. Saikat Biswas

June 20, 2018

# Contents

<b>1</b>	<b>Introduction</b>	<b>1</b>
1.1	Introduction to detectors . . . . .	1
1.2	Classification of Detectors . . . . .	2
1.2.1	Gas Filled Detectors . . . . .	2
1.2.2	Scintillation Detectors . . . . .	5
1.2.3	Semiconductor Detectors . . . . .	6
1.3	Project Aim/Scope/Objective . . . . .	6
<b>2</b>	<b>Electronic Modules</b>	<b>8</b>
2.1	Intoroduction . . . . .	8
2.2	NIM BIN . . . . .	8
2.3	Basic Module . . . . .	9
2.3.1	High voltage power supply . . . . .	9
2.3.2	Pre-amplifier . . . . .	9
2.3.3	FAN in FAN out . . . . .	10
2.3.4	Discriminator . . . . .	10
2.3.5	Digital storage oscilloscope . . . . .	10
2.3.6	Scalers . . . . .	11
<b>3</b>	<b>Resistive Plate Chamber</b>	<b>12</b>
3.1	Introduction . . . . .	12
3.2	Working principle of RPC . . . . .	14
3.3	Modes of operation . . . . .	15
3.4	RPC gas and surface finish of the electrode . . . . .	16
3.5	Different types of RPC . . . . .	17
3.5.1	Classification by application . . . . .	17
3.5.2	Classification by design . . . . .	17
<b>4</b>	<b>RPC with low resistive plates</b>	<b>21</b>
4.1	Introduction . . . . .	21
4.2	Specification of the RPC . . . . .	22

4.3	Measurement of bulk resistivity and surface resistivity . . . . .	22
4.4	Fabrication of the RPC . . . . .	23
4.5	Cosmic ray test set up . . . . .	26
4.6	Results in avalanche mode . . . . .	28
<b>5</b>	<b>Summary and outlook</b>	<b>31</b>

# List of Figures

1.1	Basic operation of gas-filled Detector . . . . .	3
1.2	Voltage response curve of detectors . . . . .	5
2.1	Electronic modules in our lab . . . . .	11
3.1	Schematic representation of a RPC . . . . .	14
3.2	Schematic diagram of a Multigap RPC . . . . .	19
4.1	Schematic diagram of the bulk resistivity measurement setup.	23
4.2	Components of the RPC . . . . .	24
4.3	Gluing of spacers is done on one plate . . . . .	24
4.4	Gluing of the second plate . . . . .	25
4.5	Complete RPC module . . . . .	25
4.6	Complete RPC module along with the pick-up strips . . . . .	26
4.7	Signal after the preamplifier. . . . .	27
4.8	Schematic diagram of cosmic ray set-up . . . . .	27
4.9	Cosmic ray set-up of our laboratory . . . . .	28
4.10	V-I characteristics. . . . .	28
4.11	Noise rate Vs. voltage. . . . .	29
4.12	Efficiency Vs. voltage. . . . .	29



# Acknowledgment

I gratefully acknowledge the constant and invaluable academic and personal support received from my supervisor Dr. Saikat Biswas. I am really thankful and indebted to him for having been the advisor everyone would like to have, for helping me to learn things in a simpler way and without whose dedicated supervision it would have been never possible to complete this project. I have really enjoyed by working with him.

I would like to thank Dr. Rajarsi Ray, for his interesting discussion and valuable suggestions during the whole M.Sc. course. He has been the substantial sources of inspirations and profound insight during these months.

I have no words to thank Dr. Supriya Das and Dr. Sidharth K. Prasad of Bose Institute for their clear and enthusiastic discussion and valuable suggestions. They have constantly motivated me throughout my study. Without their support it was very difficult to pursue this work.

I am very much indebted to some scientists at Bose Institute especially, Prof. Debapriyo Syam, Prof. Swapan K. Saha, Dr. Sandhya Dey and Dr. Atanu Maulik for their encouragement, support, collaboration and for constantly motivating me in my project work.

I would also like to thank my seniors Ms Shreya Roy for helping me in all possible ways to analyze the results of my experiments. I would like to thank Mr. Sayak Chatterjee, Abhi Modak and Prottoy Das for their valuable comments and suggestions during the weekly meeting. I would also like thank all the Bose institute staff members specially Mr. Sourav Roy for helping me in my project.

This work is also partially supported by the re-search grant of CBM-MUCH project from BI-IFCC, Department of Science and Technology, Govt. of India.

Sayan Chakraborty  
Kolkata, India

## Abstract

Resistive Plate Chamber (RPC) is one of the most widely used detector technologies for trigger and tracking in the high energy physics experiments. RPC's are usually built with high resistive glass or bakelite with a resistivity of the order of  $10^{10} - 10^{12} \Omega\text{-cm}$ . Now a days low resistive material are being explored for high rate capability ( $1\text{kHz}/\text{cm}^2$ ).

In the muon detection system (MUCH:MUON CHAMBER) of compressed baryonic matter (CBM) experiment at FAIR (Facility of Antiproton and Ion Research), Germany. Gas electron multiplier (GEM) will be used in the 1<sup>st</sup> and 2<sup>nd</sup> stations. From simulation it has been found that given the interaction rate of 10 MHz, particle flux on the 3rd and 4th stations of the CBM-MUCH has been found to be  $\sim 15 \text{ kHz}/\text{cm}^2$  and  $\sim 5.6 \text{ kHz}/\text{cm}^2$ , respectively, for central Au-Au collisions at 8 AGeV. Single gap RPC is a strong candidate for the 3rd and 4th stations of CBM-MUCH. To cope-up with this particle rate the RPC are to be built with low resistive plates and to be operated in the avalanche mode. It is planned to build a prototype single gap RPC with a low resistive material. Usage of electrodes made with low bulk resistivity seems to be a promising way to adapt the RPC to the high-rate environment of the upcoming CBM experiment. The basic characteristic study of the chamber has been carried out. the detail fabrication process and the 1<sup>st</sup> test results are discussed in this report.

# Chapter 1

## Introduction

### 1.1 Introduction to detectors

Nuclear radiation detectors or radiation detectors or simply detectors play an important role in all nuclear physics and high energy physics experiments. Nuclear radiation is a general term and it includes variety of energetic particles like electrons, protons, alpha particle, heavy ions or neutral radiations like neutrons, X-ray or gamma ray, etc. The development of radiation detectors started with discovery of radioactivity photosensitive by Henry Becquerel in 1896. He noticed that the radiations emitted by uranium salts blacken photosensitive paper. Almost at the same time Roentgen discovered X-ray. X-ray were also found to blacken photosensitive paper. So, the first radiation detector was a photosensitive paper or X-ray film and was extremely simple. In the beginning of the century, flashes Rutherford used flashes of light or scintillations produced in ZnS as nuclear radiation detector. These simple detectors used at that time were very primitive. They could simply indicate the presence or absence of radiations.

Now a days, it is not sufficient only to detect the presence or absence of radiation but one would also like to know the nature of radiations, i.e. whether the radiations are electrons, protons, alpha particles, X-ray, gamma rays etc. On top of that, accurate energy and momentum measurements are often required. In some applications an exact knowledge of the spatial coordinates of the particles trajectories is also interest.

There are number of ways in which we can classify the detectors. One simple way of classifying various detectors is by what type of signal is provided by the detector. This signal can be an electrical signal or visible light, correspondingly we classify detectors as electrical, which are based on ion collection

or optical which are based on the visible light emitted detector or form the image of the trajectory of charged particle.

## 1.2 Classification of Detectors

Detection of radiation is possible because the interaction of radiation with matter, photons, electron-ion pairs, or electron-hole pairs can be produced. The detectors which depend on the detection of the free charge carriers are usually classified under the general category of ionization based detectors. Gas filled detector and semiconductor detector belong to this category. The detectors producing the luminescence photons in the interaction called scintillation detectors.

### 1.2.1 Gas Filled Detectors

Gas-filled detectors are the oldest and most widely used detectors for nuclear radiation detection. They are based on the principle of ionization and excitation caused by charged particles while passing through the gas. A schematic diagram of a gas-filled detectors is shown in Fig. 1.1

A simple model with only two essential parts, a chamber filled with a gas (hence the term gas-filled detector ) and a basic electric circuit, is used to illustrate the operation of Gas-filled detectors. The chamber consists of a positively charged plate, anode and a negatively charged plate cathode. This anode and cathode are separated and are connected to an external power supply. The power source keeps the anode and cathode charged with as much positive and negative charge, respectively, as their size and the power sources voltage allows.

In the absence of radiation interactions, the gas between the anode and cathode acts as an insulator, and there is no movement of electrical charge. When radiation (gamma rays, X-rays, or charged particles) passes through the gas, it ionizes gas molecules, producing free electrons and positive ions.

The average amount of energy required to cause an ionization depends on the type of gas used in the chamber, but is generally between 20 and 45 eV per ion pair. The free electrons and positive ions drift towards the anode and cathode, respectively. Electrons move much faster than the positive ions they leave behind, so we can discuss the collection of electrons at the anode, ignoring for the moment the positive ions created by the radiation interac-

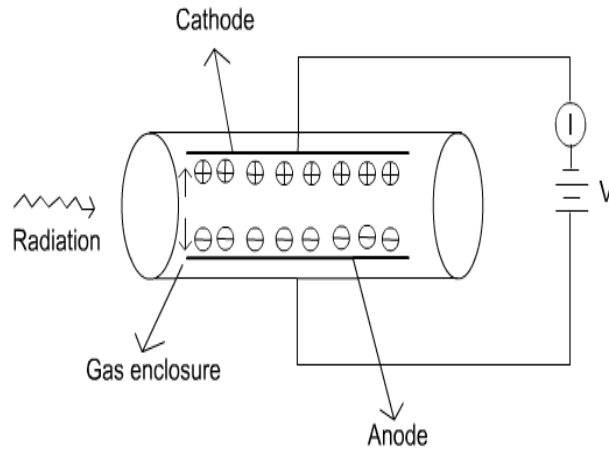


Figure 1.1: Basic operation of gas-filled Detector

tions. Electrons that reach the anode neutralize some of the positive charge, thus causing electricity to flow through the connecting circuitry to restore the capacitor to its original state. We can measure this neutralization as either current (current mode) or voltage (pulse mode).

The electrical potential difference between the anode and cathode provides the driving force behind the movement of the electrons, its magnitude determines how many reach the anode and cathode and what happens to them along the way. For now, let us leave aside the effects of energy, geometry, and gas composition, and look at the effect of changing the voltage between the anode and cathode.

### Voltage Response Curve

The applied voltage between the anode and cathode is the most important determinant of how many electrons are measured. Figure 1.2 shows a typical voltage response curve. Its shape can be understood by looking at what is happening in each of the six regions.

### Recombination Region

If the applied voltage is quite low, the electrons are moving so slowly that they recombine with the positive ions of other ionized gas molecules and do not reach the anode and cathode, resulting in an incomplete collection of ions. There are no usable detectors that operate in this region of the voltage response curve.

## **Ionization Region**

As the applied voltage is increased, the system reaches a point at which all the primary electrons are being collected, with no recombination. The saturation voltage is a voltage sufficient for this saturation point to be reached. There is a wide range over which the response is flat, so that even if the voltage fluctuates, the same number of electrons will be collected. Ionization chambers are operated in this region.

## **Proportional Region**

The electrons resulting from radiation interactions are easily accelerated by application of a higher voltage, giving them enough kinetic energy so they cause secondary ionizations through collisions with gas molecules. An increase in the applied voltage thus produces a signal that is larger than, but still proportional to, the number of ion pairs produced by the radiation or the number of secondary electrons are proportional to the number of primary electrons giving a proportionality between the pulse height and the deposited energy. This process is called gas amplification. Gas-filled detectors that operate in this region, called proportional counters, are primarily used to detect and distinguish between alpha and beta particles to identify radionuclides based on these decay products and to measure the energy. Presently all micro pattern gaseous detectors such as Gas electron Multiplier, Micromegas are operated in this region.

## **Limited of Proportional Region**

It is the region where we must begin to consider the fate of the positive ions created by the interaction of radiation with gas molecules. These ions are much heavier than electrons, and hence drift slowly toward the cathode. In this voltage range, each interaction produces a cloud of positive ions that takes a finite amount of time to disperse. The electric field experienced by the electrons is momentarily decreased, leading to a decrease in the gas amplification. Thus the voltage-response curve no longer changes linearly with increasing voltage.

## **Geiger Muller Region**

At very high voltages, the gas amplification effect is maximized, so that each electron created produces many ionizations as it races toward the anode. In addition, the moving electrons raise many other gas molecules to excited states via collision interactions, from which they may de-excite by emission of ultraviolet (UV) photons. These UV photons can interact with other gas molecules via photoelectric interactions, producing more free electrons,

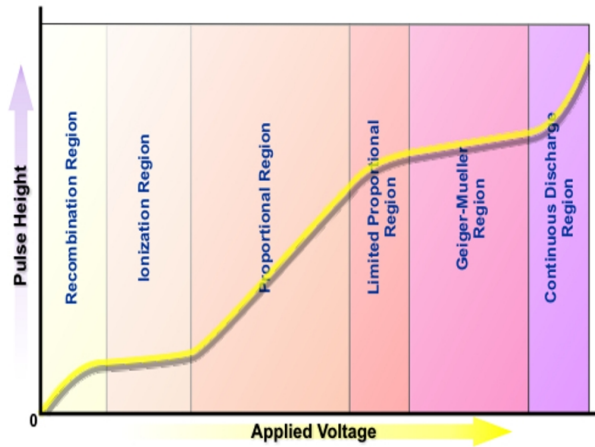


Figure 1.2: Voltage response curve of detectors

which in turn are accelerated toward the anode and cause more ionizations and excitations. Thus, each radiation event produces an avalanche of ions throughout the chamber. The circuit in this case produces a large electrical pulse in response to each radiation event, regardless of the applied voltage (within the Geiger Muller range) or the energy of the radiation. The pulse size is essentially the same for all the radiation events, no matter the type of radiation or the amount of energy transfer. The Geiger counter, a commonly used radiation detector, operates in this region.

### Continuous Discharge Region

An increase in the voltage above the Geiger Muller voltage range causes spontaneous ionizations in the detector in the absence of radiation. There are no useful radiation detectors here; operation of a radiation detector in the continuous discharge region can result in permanent damage to the detector.

## 1.2.2 Scintillation Detectors

In scintillation detectors, radiation-induced excitation produces light quanta (photons). A scintillation counting system consists of a scintillator material, a photo-multiplier tube (PMT), a power supply, and an amplifier-analyzer-scaler system. When an ionizing radiation passes through the scintillator material, it produces photons. The number of photons produced is proportional to the energy deposited in the scintillator. The scintillator is covered with a reflector except on the side which is connected to the PMT. The PMT has a photoelectric film (usually coated onto the photomultiplier tube) as its first element. When light falls on it, electrons are released by the

photo-electric effect. The number of electrons produced is proportional to the number of photons falling on the photocathode. The electrons produced are focused onto the first dynode. The dynodes are coated with a material like Cesium antimonide so that, when high-energy electrons hit them, secondary electrons are produced and hence electron multiplication occurs. A typical photomultiplier has ten or more dynodes. Electrical potential is applied between the dynodes and secondary electrons are produced in preceding dynodes gain energy before they strike the next dynode and produce more secondary electrons. A voltage divider chain is used to provide gradually increasing potential to the dynodes. Finally a large number of electrons are collected at the anode giving a signal.

### **1.2.3 Semiconductor Detectors**

The operation of a semiconductor detector is analogous to the operation of an gas ionization chamber. In an ionization chamber the incident radiation produces positive ions and electrons and an electrical signal is obtained by collecting these ions and electrons. In a semiconductor counter the incident radiation produces electrons and holes and information about the radiation is obtained by collecting them. One major difference of course is that only 3.5 eV is needed to produce an electron-hole pair in a semiconductor, while the value is  $\sim 30$  eV in an gas ionization chamber. The lower energy increases the number of electron-hole pairs per MeV of radiation and decreases the relative statistical variation in this number. Hence the energy resolution is improved and for this reason semiconductor detectors are used for energy spectroscopy of nuclear physics experiment.

The number of electron-ion pairs, photons, or electron-hole pairs depends on the fraction of the energy of the radiation deposited in the sensitive volume, on the properties of the material, and sometimes on the nature of the radiation. In the design of detectors and in the analysis of information obtained from them, it is important to know how fast the radiations deposited their energy in a medium, how much of it goes into producing electron-ion pairs, photons, or electron-hole pairs, what is the relationship between the number of ions and the energy, and how much material is needed to stop a radiation of a given energy.

## **1.3 Project Aim/Scope/Objective**

The Compressed Baryonic Matter (CBM) experiment at the future Facility for Antiproton and Ion Research (FAIR) in Darmstadt, Germany is designed



to explore the QCD phase diagram in the region of moderate baryon densities. With CBM we will enter a new era of nuclear matter research by measuring rare diagnostic probes never observed before at FAIR energies, and thus CBM has a unique discovery potential. This will only be possible with the application of advanced instrumentation, including highly segmented and fast gaseous detectors. Keeping in mind the high interaction rate of FAIR, the Muon Chamber (MUCH) detector in CBM will use Gas Electron Multiplier (GEM) in the first two stations. Given the interaction rate of 10 MHz the expected particle flux on the first station will be about  $3.1 \text{ MHz}/\text{cm}^2$ . Maximum particle flux on the 3rd and 4th stations of the MUCH have been estimated to be  $15 \text{ kHz}/\text{cm}^2$  and  $5.6 \text{ kHz}/\text{cm}^2$ , respectively, for central Au-Au collisions at 8 AGeV. We are exploring the possibility of using RPCs for the 3rd and 4th stations of CBM-MUCH.

# Chapter 2

## Electronic Modules

### 2.1 Introduction

In this section we will discuss the methods used to extract information from the pulses produced by radiation detectors. A functional or black box approach will be taken to most of the electronic components. The two most common nuclear instrumentation standards are : NIM and CAMAC. The first (and simplest) standard established for nuclear and high energy physics experiments is a modular system called NIM (Nuclear Instrumentation Module). In this system, the basic electronic apparatus, for example, amplifiers, discriminators, etc, are constructed in the form of modules according to standard mechanical and electrical specifications. These modules, in turn, fit into standardized bins which supply the modules with standard power voltages. Any NIM module will fit into a NIM bin.

### 2.2 NIM BIN

The standard NIM bin is constructed to accept up to 12 single-width modules or a lesser number of multiple-width modules. The external bin dimensions are such as to allow mounting in 19-inch racks or cabinets. The rear power connectors must provide, at the very least, four standard dc voltages, -12 V, + 12 V, - 24 V and + 24 V, as designated by the NIM convention. However, many bins also provide - 6 V and + 6 V. Prior to 1966, these voltages were not officially part of the NIM standard, but in the past decade their use has become so increasingly common that they are essentially standard now.

## 2.3 Basic Module

The NIM Bin and modules can be of two standard heights: 5.25 inches (133 mm) or 8.75 inches (222 mm), but the larger of these sizes is by far the more common. They can, however, also be built in multiples of this standard, that is, double-width, triple-width.

### 2.3.1 High voltage power supply

High voltage power supply is very important for any detector laboratory. High voltage power supply is used to bias any kind of detector. Sometimes multichannel power supply is required for a single detector. It basically consists of a step-up transformer that generates the required high voltage to bias the detector. Different detectors require different biasing voltages in the range of a few hundred volts to a few kV. For example GEM is operated as a voltage 3 - 4 kV, RPC is operated at 8 kV etc. Any desired voltage can be set in the module. The ramp up and ramp down voltages can also be set. The bias current can also be monitored from the power supply. In this present work CAEN N-1470 quad programmable module is used having 4 channels. 0-8kV voltage can be applied to a detector using it. Polarities can be changed for each channel.

### 2.3.2 Pre-amplifier

The basic function of a preamplifier is to perform impedance matching between detector output and electronics. The preamplifier is not designed to give high gain and usually its gain is of the order of  $1-10^2$  to amplify weak signals from a detector and to drive it through the cable that connects the preamplifier with the rest of the equipment. At the same time, it must add the least amount of noise possible. Since the input signal at the preamplifier is generally weak, preamplifiers are normally mounted as close as possible to the detector so as to minimize cable length. Three basic types of preamplifier are:

- 1) voltage sensitive,
- 2) current sensitive,
- 3) charge sensitive.

In this work VV50-2 charge sensitive preamplifier is used having a gain of 2 mV/fc and shaping time 300 ns.

### **2.3.3 FAN in FAN out**

Fan-outs are active circuits which allow the distribution of one signal to several parts of an electronics system by dividing the input signal into several identical signals of the same height and shape. This should be distinguished from the passive pulse splitter which divides both the signal and its amplitude. The fan-in, on the other hand, accepts several input signals and delivers the algebraic sum at the output. These modules may be bipolar, i.e., accepting signals of both polarities, or of single polarity, i.e., accepting signals of one polarity only. Fan-ins are particularly useful for summing the outputs of several detectors or the signals from a large detector with many PM's. Both fan-ins and fan-outs come in two varieties: linear and logic. The linear modules accept both analog and logic signals, whereas logic fan-outs and -ins are designed for logic signals only. In the case of a logic fan-in, the algebraic sum is replaced by a logical sum (i.e., OR). In the current work CAEN module N625 is used.

### **2.3.4 Discriminator**

The discriminator is a device which responds only to input signals with a pulse height greater than a certain threshold value. If this criterion is satisfied, the discriminator responds by issuing a standard logic signal; if not, no response is made. The value of the threshold can usually be adjusted by a helipot or screw on the front panel. As well, an adjustment of the width of the logic signal is usually possible via similar controls. The most common use of the discriminator is for blocking out low amplitude noise pulses from photomultipliers or other detectors. Good pulses, which should in principle be large enough to trigger the discriminator, are then transformed into logic pulses for further processing by the following electronics. In this role, the discriminator is essentially a simple analog-to-digital converter. In the current work CAEN 8 CH LED module N840 is used.

### **2.3.5 Digital storage oscilloscope**

To visualize the signal produced by the detector and study various characteristics of the pulse, such as rise time, fall time, pulse height, pulse shape, etc. Digital storage oscilloscope (DSO) is used. In the DSO one can set trigger and threshold to select only useful events. The DSO used in this experiment is from Agilent Technologies and can support up to four different input signal ports. In the current work DSO6054A module is used.

### 2.3.6 Scalers

The scaler is a unit which counts the number of pulses fed into its input and presents this information on a visual display. So-called blind scalers are those which do not have their own integrated display. Their contents may be read by a computer or fed into a separate display unit. In general, scalers require a properly shaped signal in order to function correctly; thus it is usually necessary to have a discriminator or a pulse shaper process signals from the detector before they can be counted by the scaler. Most commercial scalers are also available with a variety of auxiliary functions such as a gate, preset count, reset, etc. In the current work CAEN module N1145 Quad scaler is used. The whole electronic modules in our lab shown in Fig 2.1



Figure 2.1: Electronic modules in our lab

# Chapter 3

## Resistive Plate Chamber

### 3.1 Introduction

In experimental high energy nuclear physics the radiation detector is a device used to detect the charged particle or electromagnetic radiation produced in high energy collision experiments or in cosmic radiation. Detectors are also used to measure energy, momentum, life time and other property of the particles produced in an experiment.

Gas filled detectors were the first measuring instrument developed for the detection of the radiation. Since gas filled detectors are cheap and simple to fabricate and to operate, these are used in all high energy physics experiments(e.g STAR, CMS,CBM, ATLAS). According to the parameters e.g. efficiency, rate, particle identification capability, time and position resolution gas filled detector can also vary. Based on the requirements, conditions are varied. Different types of gaseous detectors presently used are Multi-Wire Proportional Counter (MWPC), Time Projection Chamber (TPC), parallel plate avalanche chamber (PPAC), Gas Electron Multiplier (GEM), Resistive Plate Chamber(RPC) etc.

The position resolution i.e. the capability of localizing particle trajectory in a small region, the time resolution i.e. how small time interval of two particles separately falling on the detector can be measured and efficiency i.e. what fraction of particles falling on it can be detected, are the important properties of the detector. In high energy physics (HEP) experiments the position resolution from  $\sim$  a few cm to  $\sim$  a few  $\mu\text{m}$  and the time resolution from  $\sim$  1-2 ns to 50 ps are necessary depending on the requirements. In some experiments high efficiency ( 95%), high rate handling capacity ( $\sim$  1

MHz/cm<sup>2</sup>) and in addition, the capability of working in high multiplicity are too much essential. Other challenges of the HEP detectors are the use of large number of cells and the cost.

Resistive Plate Chamber (RPC) is a gas filled detector utilizing a constant and uniform electric field produced between two parallel electrode plates made of a material with high bulk resistivity e.g. glass or bakelite. Since such a detector has very good timing ( $\sigma \sim 1\text{-}2$  ns) and spatial resolution, it is very suitable for a tracking calorimeter. The first resistive spark chambers were developed by Fedotovitch et al. He used semi-conductive glass and a gas gap of 100  $\mu\text{m}$ . Then a planar chamber with gaps of 1.52 mm, simple in construction and having gas mixtures at atmospheric pressure was developed. This technique, although economical, had few difficulties in operation at that time. To overcome some of these difficulties developed a new type of RPC based on low cost resistive glass plate electrodes was developed by Anelli et al. The RPCs are made up of highly resistive (bulk resistivity  $\sim 10^{10}\text{-}10^{12}\Omega\text{-cm}$ ) plates (e.g. glass, bakelite etc.) as electrodes, which help to contain the discharge created by the passage of a charged particle or an ionizing radiation in a gas volume, and pick-up strips are used to collect the resulting signals. Typical time resolution for a single gap RPC is  $\sim 1\text{-}2$  ns. By reducing the gaps between the electrodes or by using multi-gap configuration, time resolution can be improved to  $< 50$  ps .

The RPCs can be operated in two modes, viz., the avalanche mode and the streamer mode . Over the years, one of the main concerns with the use of RPCs is their long term stability. In the avalanche mode, the amount of charge which is produced in the gas is small and it allows the RPC to recover in a relatively shorter time to handle high counting rates ( $\sim 1$  kHz/cm<sup>2</sup>). In this mode, the ageing effects caused by the accumulated charge is also relatively less. But for the case of streamer mode, produced charge amount is considerably larger creating induced signals of larger magnitude. So the recovery time is also larger and the irreversible damage caused by the accumulated charge reduces the life of the RPC. However, several remedial measures can be taken to prolong its lifetime under streamer mode of operation. Careful choice of materials, smoothness of surfaces to avoid localization of excess charges, surface treatment to reduce the surface resistivity recovery are adopted in the major high energy physics experiments. The main advantage of the streamer mode is that it needs relatively less number of electronic components. Mainly for low rate applications the glass-based RPCs are found to be more stable. However, in the avalanche mode of operation, the de-

tectors can be operated for longer periods. At the end of nineties, it was found that the RPCs based on bakelite with linseed oil coating show serious ageing effects reducing the efficiency drastically in particular at high rate. It has however been found that for several ongoing and future applications (e.g CBM experiments) relatively low resistive plate based RPCs are chosen as preferred options mainly due to cheaper cost of fabrication and easy to handle.

### 3.2 Working principle of RPC

A single gap RPC, shown in Figure is made of two parallel electrode plates with high bulk resistivity of the order of  $10^{10}$ - $10^{12}$   $\Omega$ -cm (e.g. Glass, Bakelite, etc) separated by spacers made of even higher resistive materials like polycarbonate. With suitable gas mixture e.g. argon, isobutane and tetrafluoroethane (R-134a) the detector is filled. To produce electric field between two resistive plates a d.c high voltage power is applied across these plates.

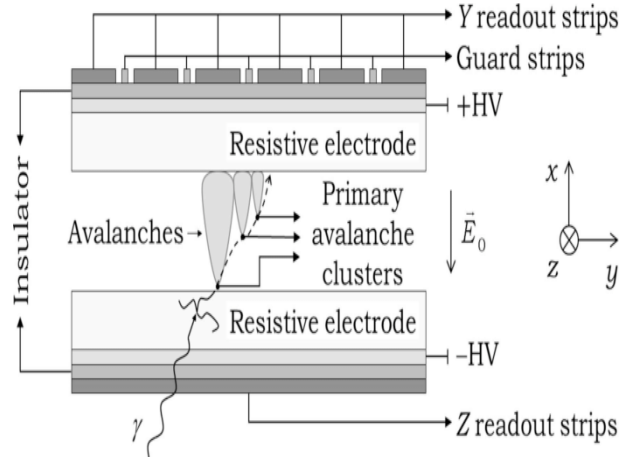


Figure 3.1: Schematic representation of a RPC

Due to high resistivity of the material charge-up process is slow. A passing charged particle induces an avalanche, which develops into a spark. The discharge stops when the local charge is used up. To prevent the secondary streamer by quenching the photon isobutane is used and R-134a is used to limit the streamer size from spreading in transverse direction. In the discharge region the electric field is reduced suddenly and the region is dead until re-charged through the bulk resistivity of the plates. Due to the high resistivity of the plates the discharge is also prevented from spreading through the whole gas. When readout strips are placed on the outer surface of the



electrodes, induced charges are either drawn in or drawn out from the readout strips, generating voltage signals of opposite polarities on the two sides of a RPC. The charge-up time after each discharge is given by

$$\begin{aligned}
\tau &= R_{bakelite} C \simeq \left( \frac{\rho_{bakelite} d_{bakelite}}{A} \right) \left( \frac{\kappa_{gas} \epsilon_0 A}{d_{gas}} \right) \\
&= \rho_{bakelite} \kappa_{gas} \epsilon_0 \\
&\simeq (5 \times 10^{10} \Omega \cdot m)(\sim 4)(8.85 \times 10^{-12}) \simeq 2 \text{ sec}
\end{aligned} \tag{3.1}$$

where  $R_{bakelite}$  and  $\rho_{bakelite}$  are respectively the resistance and the bulk resistivity of the bakelite plate and  $C$  is the chamber capacitance. Here the thickness of the bakelite plate ( $d_{bakelite}$ ) and the gas gap ( $d_{gas}$ ) are same.  $\kappa_{gas}$ ,  $\epsilon_0$  and  $A$  are the dielectric constant of the gas, permittivity of free space and the area of the chamber respectively.

Each discharge is localized to  $\sim 0.1 \text{ cm}^2$ . Therefore, RPC with  $0.2 \text{ Hz/cm}^2$  count rate suffers dead time fraction of  $0.2 \times 0.1 \times 2 = 0.04^1$ . So one should aim to build and operate RPC with less than  $0.2 \text{ Hz/cm}^2$  in order to keep the dead time fraction below 5%.

### 3.3 Modes of operation

The RPCs are operated in two modes, viz., the streamer mode and the avalanche mode. These two modes are explained below.

Let  $n_0$  be the number of electrons in a cluster at any particular point inside the gas gap. If  $\alpha$  is the first Townsend coefficient i.e. the number of ionisations per unit length and  $\beta$  is the attachment coefficient i.e the number of electrons captured by the gas per unit length then the number of electrons reaching the anode,

$$n = n_0 e^{(\alpha - \beta)x}$$

where  $x$  is the distance between anode and the point where the cluster is produced. The gain of the chamber is defined by

$$M = n / n_0$$

---

<sup>1</sup>The dead time fraction is calculated as:

$$\frac{0.2 \text{ particles}}{\text{cm}^2 \text{ sec}} \times 0.1 \text{ cm}^2 \times 2 \text{ sec}$$

So, 0.04 particles in each discharge is lost.

the mode of operation of the RPC depends on the gain  $M$ . If  $M > 10^8$  the mode is called the streamer mode and if  $M \ll 10^8$  the mode is avalanche mode. In streamer mode of operation, the efficiency of the RPC decreases quickly with the rate since the surface of the resistive plates becomes charged and reduces the electric field across the gas gap. The full electric field is restored by current flowing through the resistive plates. A possible way to handle high rate is to operate the RPCs in avalanche mode using some sensitive preamplifiers. But there are some possibilities of discharge in avalanche mode too, which can cause of damage of the preamplifiers. To reduce the effect of sparks there are basically two methods. The first one is to quench the spark by using a high fraction of u.v. photon-absorbing gas, such as isobutane. The second method is the size of the gas gap can be increased which decreases the probability of a spark.

### 3.4 RPC gas and surface finish of the electrode

In the RPC a gas of a high absorption coefficient for ultraviolet light is filled between the two electrodes. A mixtures of argon with isobutane in widely varying ratios are used in the streamer mode of operation whereas in the avalanche mode mostly use mixtures of tetrafluoroethane with 2-5% of isobutane. , Sometimes a small fraction of  $SF_6$  is also used as quencher in the avalanche mode to reduce streamer fraction. When the gas is ionized by a charged particle crossing the detector a discharge is originated by the electric field. The discharge, however, is prevented from propagating through the whole gas because, due to the high resistivity of the electrode plates, the electric field is suddenly switched off in a limited area around the point where the discharge occurred. The sensitivity of the chamber remains unaffected out of this region . On the other hand, due to the ultra-violet absorbing component of the gas (*iso* –  $C_4H_{10}$ ), the discharge photons are not allowed to propagate in the gas, thus avoiding the possibility to originate secondary discharges in other points of the detector. R-134a is used as electron quencher i.e. to limit the streamer size from spreading in transverse direction. For steady operation of the RPC smooth inner surface is an important factor. Due to surface roughness, particularly the sharp pin like edge in the surface morphological structure the electric field inside the RPC may vary  $\sim 5 - 12\%$ . Rough surface is very sensitive to the field emission which is a source of high dark current and high counting rates. That is why rough inner surfaces of the bakelite electrodes were coated by 2-propanol (or similar chemical solution)

diluted Linseed oil, otherwise its huge noise rate prohibits the chamber from any practical application. Another point is that the photoelectric efficiency is enhanced by the strong electric field presented on the surface of the RPC. In every avalanche or streamer the UV photon is created which can hit the large surface of the cathode. The material for the electrode must be least UV sensitive to reduce the after pulse / noise rate. HF, produced by fluorine with the interaction of water vapour is notoriously chemical reactive, it can attack many different materials and has corrosive action. From several tests it is proved that the Linseed oil coating on Bakelite surface can effectively protect the surface from HF vapour attack.

## **3.5 Different types of RPC**

### **3.5.1 Classification by application**

According to the application, RPCs are classified into two categories:

1. Trigger RPC
2. Timing RPC.

#### **Trigger RPC**

The type of RPC used for triggering the Minimum Ionising Particles (MIPs) such as muons in the muon detector systems are referred to as the Trigger RPC. Single gap (gas gap  $\sim 2$  mm) or double gap RPCs with large area, operated in streamer or avalanche mode are used for trigger RPC. These types of RPCs provide an efficiency  $>95\%$  with a time resolution of  $\sim 1-2$  ns ( $\sigma$ ).

#### **Timing RPC**

Resistive Plate Chambers with large area and with gas gaps of 0.2 to 0.3 mm are widely used in multi gap configurations for Time-Of-Flight (TOF) measurements. These type of RPCs are operated in avalanche mode with an electric field of 100 kV/cm. The efficiency of this type of RPC is  $\sim 99\%$  with a time resolution of  $\sim 100$  ps ( $\sigma$ ) or better. The time resolution is the most important factor for timing RPC.

### **3.5.2 Classification by design**

According to their design there are several types of RPC. A brief description of various designs of RPC is given below.

## Single-gap RPC

The single gap RPC, first developed by R. Santonico and R. Cardarelli which is basically a charged particle detector consisting of two parallel plates electrodes made of high resistive material such as bakelite or glass (bulk resistivity  $\sim 10^{10} - 10^{11} \Omega\text{-cm}$ ) enclosing a gas volume. A uniform gap of 2 mm is maintained by spacers made by a material such as polycarbonate whose resistivity is much higher than the resistivity of the electrode plates. An electric field is produced across the gas gap between two electrode, by applying a d.c high voltage to these electrodes. A passing charged particle creates an avalanche in the gas. Due to the high resistivity of the plates the discharge is prevented from spreading through the whole gas. The signal on the pickup strips is induced by the created electron and positive ion pairs while traveling towards the respective plates. The generated charge is deposited on a small region of the electrode plate; this spot is slowly recharged by current flowing through the plate. If the electric field is even more intense, there is a possibility of 'spark' in the avalanche mode.

In the conventional single gap RPC a gas mixture of argon, isobutane and tetrafluoroethane (R134a) in widely varying proportions is used at atmospheric pressure in the streamer mode of operation. The secondary streamer by quenching the photon is prevented by using the isobutane, and R134a is used to limit the streamer size from spreading in transverse direction. In the avalanche mode of operation a mixtures of tetrafluoroethane (R134a) with 2-5% of isobutane are used. The single gap RPC first developed has been replaced by its variants such as electrode materials, gap thickness and geometry etc.

## Wide-gap RPC

In the RPC the gas gap is used for two purposes,

- 1.To produce the primary ionisation cluster
- 2.For the gas gain.

The accumulated charge in a RPC signal depends on the gas gap. Two types of detector can be used, the first one is single (gas gap:  $\sim 2$  mm) gap RPC (sometimes it is called as narrow gap RPC) and the second one is wide gap RPC (gas gap: 8 mm or 9 mm). Lower dynamic range of signal is the main advantage of the wide gap RPC ; this leads to the smaller current flowing through the gas gap and resistive plates. Wide gap helps to produce large signal amplitude particularly in avalanche mode. As larger path produces larger fluctuation in signal arrival time the time resolution is poor for this case.

## Multi-gap RPC

The Multi-gap Resistive Plate Chamber (MRPC) which is operated at atmospheric pressure and consists of several small gas gaps (0.2 mm to 1 mm for each step). Small gap improves the time resolution. In MRPC the total gas volume is divided into a number of small gas gaps with equal width by inserting intermediate resistive plates (bulk resistivity  $\sim 10^{11} - 10^{12} \Omega\text{-cm}$ ) between the two outermost resistive plates. The high voltages (HV) are applied only to the external surfaces of each stack of plates and the intermediate plates are electrically floating, thus one can build the detector by stacking plates separated by suitable spacers. Pickup strips are located outside the stack and insulated from the high voltage electrodes. A passing charged particle creates an avalanche in the gas. Signals on the pickup electrodes are induced by the movement of charge in the gas; in case of the RPC, the fast signal is generated by the fast movement of electrons towards the anode. Since the resistive plates act as dielectrics, the induced signals can be caused by the movement of charge in any of the gas gaps between the anode and the cathode pickup strips. In this way the observed induced signal on the pickup strip becomes the sum of the individual avalanche signal in any of the gaps

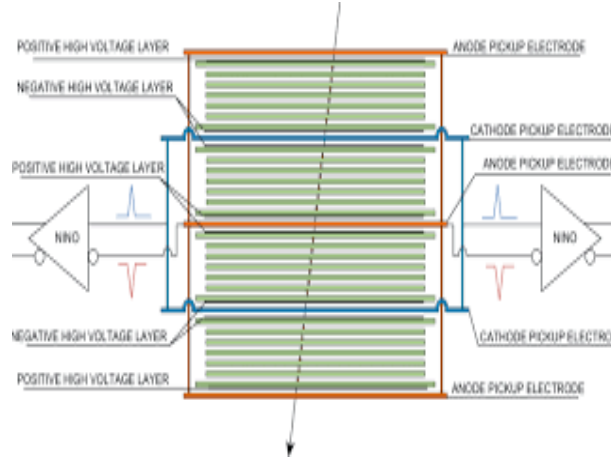


Figure 3.2: Schematic diagram of a Multigap RPC

making up the MRPC, but the time jitter in the rise time is expected to reduce due to the smaller sub gap of the MRPC. It is shown by simulation that efficiency increases and time resolution improves with the increase of number of gap. Though for a multi-gap RPC of  $n$  number of gaps the time resolution does not scale with  $\sigma_t/\sqrt{n}$ , however, the efficiency does scale with  $1 - (1 - \epsilon)^n$ , where  $\sigma_t$  and  $\epsilon$  are the time resolution and efficiency respectively of the single gap RPC. The schematic diagram of 24 gap RPC is shown in

Fig 3.2. It shows detector is divided into four stacks, each with six gas gaps of  $160\text{ }\mu\text{m}$ . The best time resolution obtained from this detector was 20 ps.

# Chapter 4

## RPC with low resistive plates

### 4.1 Introduction

Single gap Resistive Plate Chamber (RPC) is one of the most widely used detector technologies for trigger and tracking in high energy physics experiments for its excellent efficiency and time resolution [1, 2, 3]. Rate handling capacity of RPC can be increased using low resistive electrode plate and operating the RPC in the avalanche mode.

Triple GEM (Gas Electron Multiplier) detectors will be used in the first two stations of the CBM (Compressed Baryonic Matter) [5] muon chamber (MUCH) at the future Facility for Antiproton and Ion Research (FAIR) [6] in Darmstadt, Germany. Given the interaction rate of 10 MHz the expected particle flux on the first station of CBM-MUCH will be about  $3.1 \text{ MHz/cm}^2$ . Maximum particle flux on the 3<sup>rd</sup> and 4<sup>th</sup> stations of the CBM-MUCH have been estimated to be  $15 \sim \text{kHz/cm}^2$  and  $5.6 \sim \text{kHz/cm}^2$ , respectively, for central Au-Au collisions at 8 AGeV. We are exploring the possibility of using RPCs for the 3<sup>rd</sup> and 4<sup>th</sup> stations of CBM-MUCH.

There are several working groups that are currently working on high rate RPC's using different materials such as Si-based Ceramics, Low-resistive Glass, low-resistive bakelite etc. A new type of single gap RPC has been fabricated using very low-resistive carbon-loaded PTFE material to compete with all these other groups and materials. In terms of bulk resistivity, this material is the lowest and should in principle be able to work at the highest rates, provided the material can withstand working bias and radiation. The chamber is tested in avalanche mode. The efficiency and noise rate of the RPC are measured with cosmic rays. The detail method of fabrication and first experimental results are presented.

## 4.2 Specification of the RPC

We have designed a prototype RPC with a carbon-loaded Polytetrafluoroethylene (PTFE) material commonly known as Teflon. This particular sample is 25% carbon-filled having a bulk resistivity of  $10^5 \Omega\text{-cm}$ . The bulk resistivity and surface resistivity of the sample have been measured using the method as described in detail in Section 4.3. It is to be mentioned here that that carbon-loaded PTFE or any other carbon-loaded resistive plate can be tuned according to the resistivity requirement by changing the carbon-content and these resistive plates can be used for high rate RPC R&D. The relationship between carbon-content and the resistivity is non-linear and substantial R&D needs to be done on this front alone to find suitable materials.

In this detector two  $15 \text{ cm} \times 15 \text{ cm}$  plates of thickness 1 mm are used to build the chamber. 2 mm gas gap has been maintained using four  $1 \text{ cm} \times 15 \text{ cm}$  edge spacers and four button spacers of 1 cm diameter. Two gas nozzles are used for gas inlet and outlet. All the spacers and nozzles are made of polycarbonate. The measured surface resistivity of the carbon-loaded PTFE has been found to be  $20 \text{ k}\Omega/\square$ . Since the surface resistivity of carbon-loaded PTFE is very low, the material has not been coated with graphite for high voltage distribution. As the surface of the material has been found to be smooth by visual inspection, we have not used oil coating in this case. The method of fabrication is discussed in Section 4.4.

## 4.3 Measurement of bulk resistivity and surface resistivity

The bulk resistivity (volume resistivity) of the electrode plates of the RPC is an important parameter that needs careful consideration for various reasons. The high resistivity helps in controlling the time resolution, counting rate and also prevents the discharge from spreading through the entire gas volume. The bulk resistivity of the sample is measured via the measurement of leakage current. Figure 4.1 shows the schematic diagram of the set up for the bulk resistivity measurement. The material sheet is taken and two  $1 \text{ cm} \times 1 \text{ cm}$  copper plates are pasted to apply voltage. Two cables were soldered on to the copper plates and were connected to the high voltage power supply and a  $110 \text{ k}\Omega$  resistance ( $R$ ) was kept in series with it. The voltage drop ( $\Delta V$ ) across  $R$  was measured with the help of a four and half digit multimeter as function of the applied voltage. The resistance ( $R_v$ ) of the bakelite sample



was obtained from the relation:

$$R_v = \frac{(AV - \Delta V) R}{\Delta V}, \quad (4.1)$$

where,  $AV$  is the voltage delivered from the high voltage supply.  $AV$  is changed from 1 V to 17 V and a resistivity of  $\sim 10^5$  was obtained.

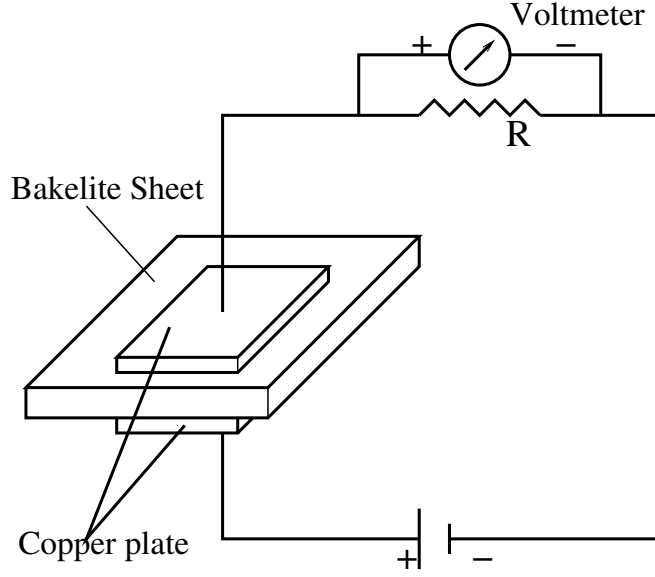


Figure 4.1: Schematic diagram of the bulk resistivity measurement setup.

To measure the surface resistivity a H-shaped aluminium jig was used. The length and separation of two aluminium bar were kept 5 cm. The separation was made using G-10 bar. The jig is placed on different part of the surface and the resistance is measured using a digital multi-meter. The surface resistivity has been found to be  $20 \text{ k}\Omega/\square$ .

## 4.4 Fabrication of the RPC

In this work RPC prototype of dimension  $(15 \text{ cm} \times 15 \text{ cm})$  has been fabricated. The components of the RPC is shown in Figure 4.2. All the components are cleaned with alcohol first. Two carbon-loaded PTFE sheets, each of thickness 1 mm have been used as electrodes. Inner surfaces of two sheets are separated by a gap of 2 mm. Uniform separation of the electrodes are ensured by using 4 button spacers of 1 cm diameter and 2 mm thickness, and

four 1 cm  $\times$  15 cm edge spacers, both being made of polycarbonate. Two nozzles for gas inlet and outlet, also made of polycarbonate, are placed at diagonally opposite corners. All the spacers and nozzles are glued to one of the PTFE sheet using Araldite epoxy adhesive. Gluing of spacers and gas nozzles on one electrode plate is shown in Figure 4.3. After gluing pressure is applied using metal clip as shown in Figure 4.3 and left for 24 hours for curing.

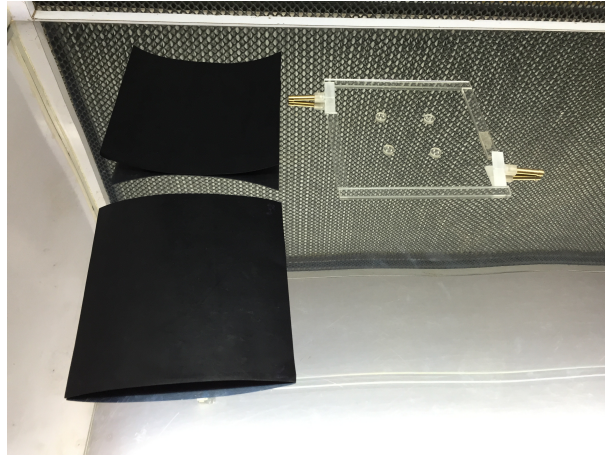


Figure 4.2: Components of the RPC

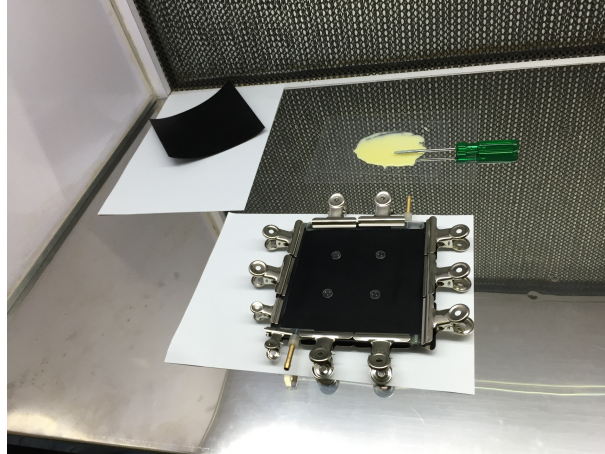


Figure 4.3: Gluing of spacers is done on one plate

Next day the second plate is glued and kept for 24 hours applying pressure. This is shown in Figure 4.4. It was ensured that the opening of the gas nozzles are not closed with glue using two metal wires.

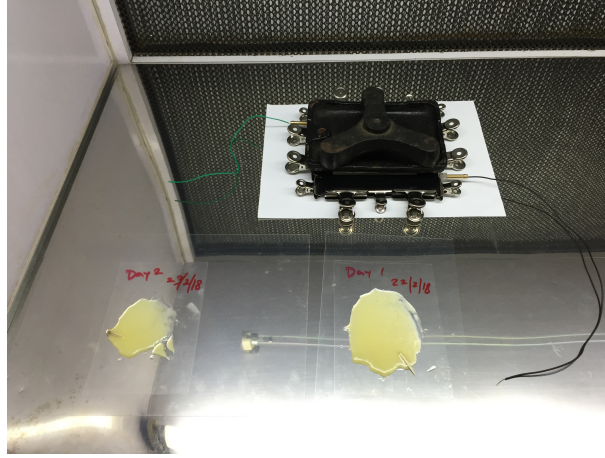


Figure 4.4: Gluing of the second plate

After curing two small ( $10\text{ mm} \times 10\text{ mm}$ ) copper tape of thickness  $20\text{ }\mu\text{m}$  are pasted by Kapton tapes on both the outer surfaces diagonally opposite to each other for application of high voltages. The high voltage cables are soldered on these copper tapes as shown in Figure 4.5.

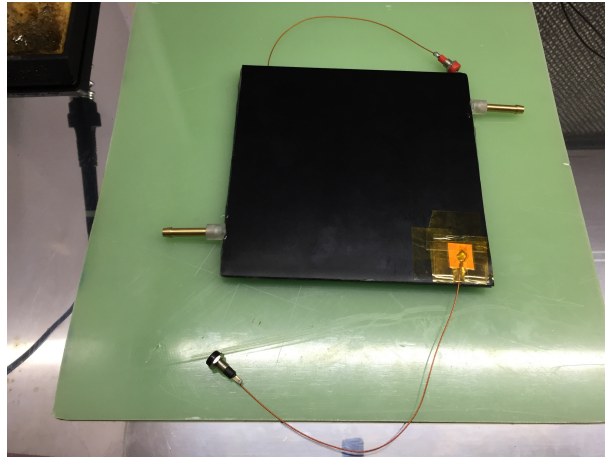


Figure 4.5: Complete RPC module

To build the capacitive pick-up strip two  $3\text{ mm}$  thick G-10 material is taken and four  $2.5\text{ cm}$  wide and  $15\text{ cm}$  long copper tape is pasted on one side keeping  $2\text{ mm}$  separation between two. The ground plane is made using aluminium foil. For signal collection  $10\text{ cm}$  long LEMO cables are fixed to each strip. The complete RPC along with the pick-up strips are shown in Figure 4.6.

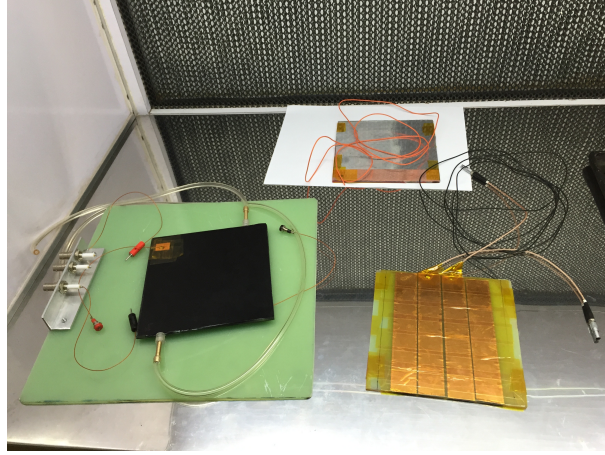


Figure 4.6: Complete RPC module along with the pick-up strips

Equal high voltages with opposite polarities are applied on both the surfaces.

## 4.5 Cosmic ray test set up

In this work 100% R-134a (Tetrafluoroethane) has been used as the sensitive gas for the chamber. The induced signal is readout by orthogonal pick-up strips placed on two sides of the chamber. As mentioned earlier there are four copper strips of dimension  $2.5\text{ cm} \times 15\text{ cm}$  with a separation of  $2\text{ mm}$ , at the central part of the module in each side.

Differential voltage (equal and of opposite polarities on two electrodes) has been applied to the chamber to produce the electric field inside the gas gap. A charge sensitive preamplifier (VV50-2) [8] with gain  $2\text{ mV/fC}$  and shaping time  $300\text{ ns}$  has been used for the signal collection. In the Figure 4.7 the Green line represents the signal after the preamplifier, which has been taken from the positive plane of the detector. There was always a reflected negative part in each signal because of impedance mismatch and this negative part has been used to discriminate the signal from noise using a leading edge discriminator (LED). Thresholds in the discriminators are optimised to reduce the noise. For efficiency measurement a cosmic ray trigger set-up is used keeping two plastic scintillator detectors of dimension  $20\text{ cm} \times 20\text{ cm}$  and  $2\text{ cm} \times 10\text{ cm}$  above the chamber and one with dimension  $10\text{ cm} \times 10\text{ cm}$  below it. Effectively an overlap area of  $2\text{ cm} \times 10\text{ cm}$  is available for triggering purpose. The coincidence signals from these three scintillator detectors are taken as master trigger and shown in Figure 4.7 (Yellow). The width of

the trigger has been set at 120 ns. The discriminated RPC signal shown in magenta in Figure 4.7 has been taken in coincidence with the master trigger to get a four-fold signal. The three-fold master trigger and the four-fold signals are counted using a NIM scaler. The un-triggered discriminated RPC signals are also counted to measure the noise rate.

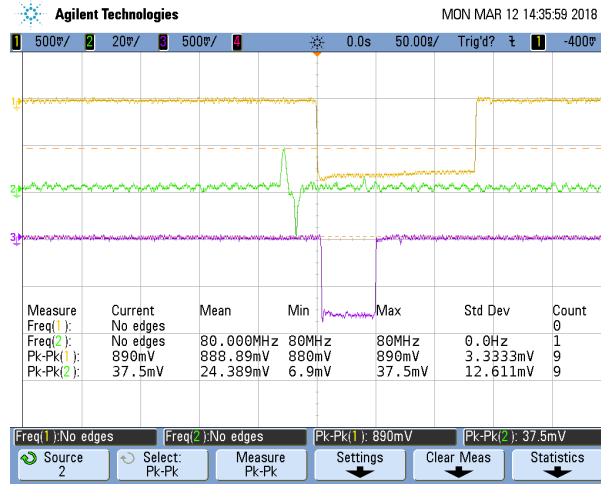


Figure 4.7: Signal after the preamplifier.

The schematic diagram of the cosmic ray test setup is shown in Figure 4.8. The actual set-up for cosmic ray with all the detectors is shown in Figure 4.9.

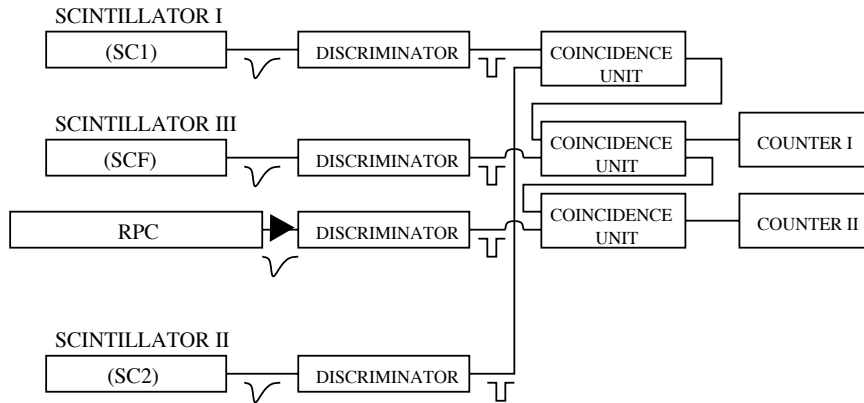


Figure 4.8: Schematic diagram of cosmic ray set-up

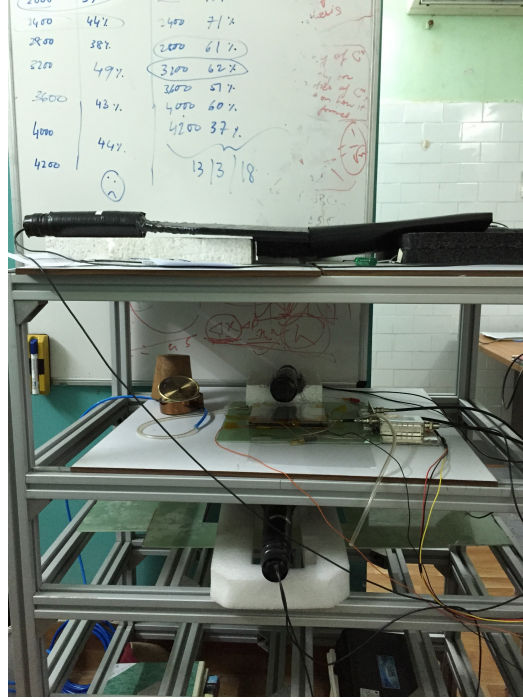


Figure 4.9: Cosmic ray set-up of our laboratory

## 4.6 Results in avalanche mode

In this study the prototype chamber has been tested for V-I characteristics, variation of noise rate and efficiency as a function of applied voltage. Equal voltages of opposite polarity have been applied on two planes of the module

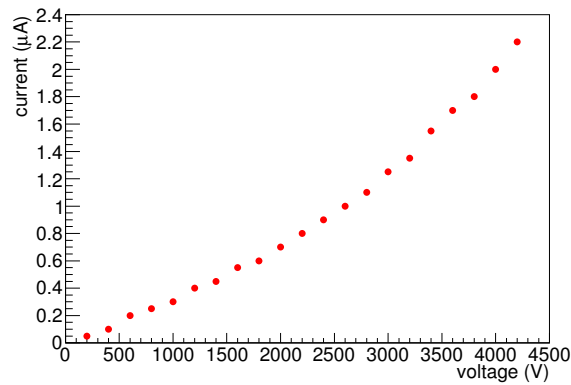


Figure 4.10: V-I characteristics.



and the leakage current has been measured. The V-I characteristics for the module is shown in Figure 4.10.

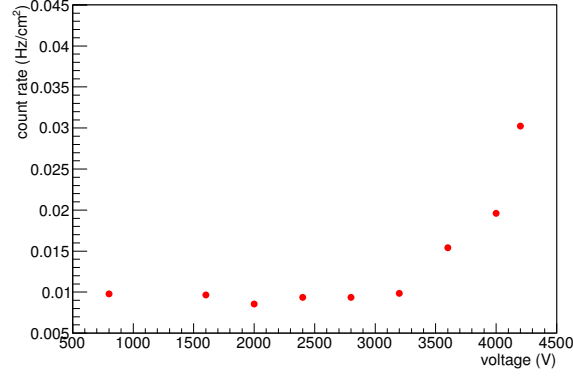


Figure 4.11: Noise rate Vs. voltage.

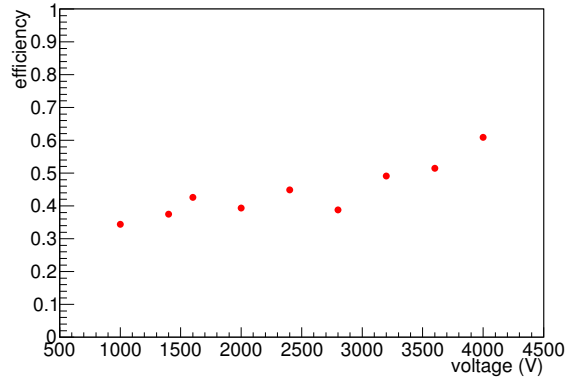


Figure 4.12: Efficiency Vs. voltage.

The three-fold signals, four-fold signals and the singles from the RPC are counted for 30 minutes for each voltage setting. The singles count rate has been divided by the area of a strip and the count rate per unit area is shown as a function of voltage in Figure 4.11. It is seen that the noise rate increases with voltage. The ratio of the four-fold count rate to the three-fold count rate is the efficiency and that as a function of voltage is shown in Figure 4.12. The efficiency increases with increasing applied voltage. At a voltage of 4 kV a typical value of efficiency and noise rate are found to be

$\sim 60\%$  and  $0.02 \text{ Hz/cm}^2$  respectively. This value of efficiency is quite low considering a typical single gap efficiency of  $90 \%$ . However for this detector discharges happen beyond the high voltage of  $4 \text{ kV}$ .



# Chapter 5

## Summary and outlook

A single gap RPC prototype has been fabricated with very low resistive carbon-loaded PTFE plate commonly known as Teflon, to improve the rate capability. The detector has been tested in avalanche mode using 100% R-134a as the sensitive gas. A charge sensitive preamplifier with gain 2 mV/fC and shaping time 300 ns has been used for signal collection. The V-I characteristics, variation of noise rate and efficiency as a function of voltage are studied. At a voltage of 4 kV an efficiency  $\sim 60\%$  is achieved.

We have worked with a sample which has 25% carbon-filled having a bulk resistivity of  $10^5 \Omega\text{-cm}$  and in the second phase of R&D a new carbon-loaded PTFE will be used with a lower carbon-filling which increases the bulk resistivity to  $\sim 10^8 \Omega\text{-cm}$ . This will allow us to operate the detector at relatively higher voltage. The long-term stability test of the modules are also in future plan.

The main goal of construction of this new type of RPC is to use it for handling high rate radiation.

# Bibliography

- [1] R. Santonico, R. Cardarelli, Nucl. Inst. and Meth. 187 (1981) 377.
- [2] S.Biswas, et al., Nucl. Instr. and Meth. A 602 (2009) 749.
- [3] S.Biswas, et al., Nucl. Instr. and Meth. A 617 (2010) 138.
- [4] Saikat Biswas et al. Performances of silicone coated high resistive bakelite RPC. arXiv:1206.5627
- [5] <http://www.fair-center.eu/for-users/experiments/cbm.html> .
- [6] <http://www.fair-center.eu/> .
- [7] K. K. Meghna et al., 2012 JINST 7 P10003 doi:10.1088/1748-0221/7/10/P10003.
- [8] CDT CASCADE Detector Technologies GmbH, Hans-Bunte-Str. 8-10, 69123 Heidelberg, Germany, [www.n-cdt.com](http://www.n-cdt.com).

### Outcome of the project

- **A new type of RPC with very low resistive plates.**  
Authors: **S. Chakraborty**, S. Chatterjee, S. Roy, A. Roy, S. Biswas, S. Das, S. K. Ghosh, S. K. Prasad, S. Raha  
Presented in **14<sup>th</sup> Pisa Meeting on Advanced Detectors, La Biodola, Isola d'Elba (Italy)**, to be published in NIM-A.
- **Study of uniformity of characteristics over the surface for triple GEM detector.**  
Authors: S. Chatterjee, **S. Chakraborty**, S. Roy, S. Biswas, S. Das, S. K. Ghosh, S. K. Prasad, S. Raha  
Presented in **14<sup>th</sup> Pisa Meeting on Advanced Detectors, La Biodola, Isola d'Elba (Italy)**, to be published in NIM-A.
- **Stability study of gain and energy resolution for GEM detector.**  
Authors: S. Roy, S. Rudra, S. Shaw, S. Chatterjee, **S. Chakraborty**, R. P. Adak, S. Biswas, S. Das, S. K. Ghosh, S. K. Prasad, S. Raha  
Presented in **14<sup>th</sup> Pisa Meeting on Advanced Detectors, La Biodola, Isola d'Elba (Italy)**, to be published in NIM-A.